

1  
2  
3  
4  
5  
6  
7  
8  
9  
10  
11  
12  
13  
14  
15  
16  
17  
18  
19  
20  
21  
22  
23  
24  
25  
26  
27  
28  
29  
30  
31  
32  
33  
34  
35  
36  
37  
38  
39  
40  
41  
42  
43  
44  
45  
46  
47  
48  
49  
50  
51  
52

## Reviewer 1

We would like to thank Reviewer #1 for his/her review of our paper and the important comments and suggestions provided. Please, find below our responses to the Reviewer's comments and the details on how we address them in the new version of the manuscript.

**1.1) Line 27: This approach has been used before so it's not accurate to call it innovative. Zhao and Weng (2002, <http://www.jstor.org/stable/26184983>) retrieved ice cloud parameters by isolating ice scattering signature. The latter is derived from observed high frequency TBs and simulated cloud base (i.e. clear-sky) TBs. They calculated the over land cloud base high frequency TBs from low frequencies with the assumption that low frequency measurements are less affected by cloud scattering. Please modify the manuscript accordingly and cite Zhao and Weng's paper.**

Thanks to the reviewer for the very useful suggestion. The HANDEL-ATMS approach is indeed very similar to Zhao&Weng's approach. However, it is also worth noticing some important differences:

- 1) the Zhao&Weng Algorithm screens out all possible "scattering surfaces" including snow cover and sea ice, that are the kind of surfaces where HANDEL-ATMS is focused on.
- 2) the Simulated clear-sky TB estimated by Zhao&Wheng is obtained by an empirical relationship between AMSU-A 23 and 31 GHz and 89 and 150 GHz clear-sky TB; in our work, an emissivity spectrum has been estimated for the ATMS channels downstream a background surface classification and the differences between the observed signal and the simulated one for 16 different channels have been used as input of a neural network approach

Moreover in the Abstract we stated:

*The main novelty of the approach is the radiometric characterization of the background surface (including snow covered land and sea ice) at the time of the overpass to derive multi-channel surface emissivities and clear-sky contribution to be used in the snowfall retrieval process.*

The statement in parenthesis, in our opinion, is sufficient to restrict the novelty of the approach to some background surfaces. Therefore we would like to keep the abstract as it is. However, we recognize the importance of the Zhao&Weng approach and the similarities between that work and HANDEL-ATMS and we modified the Introduction (lines 99-121):

From:

*The main novelty of the approach is the exploitation of the ATMS wide range of channels (from 22 GHz to 183 GHz) to obtain the radiometric characterization of the background surface at the time of the overpass. The derived surface emissivities are used to infer the clear-sky contribution to the measured TBs in the high frequency channels in the snowfall retrieval process. Moreover, the algorithm is based on the exploitation of an observational dataset where each ATMS multichannel observation is associated with coincident (in time and space) CloudSat CPR vertical snow profile and surface snowfall rate (hereafter ATMS-CPR coincidence dataset). Several snowfall retrieval algorithms for cross-track scanning radiometers have evolved in the last 20 years starting from the Advanced Microwave Sounder Unit-B (AMSU-B) (Kongoli et al, 2003, Skofronick-Jackson et al, 2004, Noh et al., 2009, Liu and Seo 2013), and Microwave Humidity Sounder (MHS) (see Liu & Seo, 2013, Edel et al, 2020), and evolving to ATMS (Kongoli et al, 2015, Meng et al, 2017, Kongoli et al, 2018, You et al, 2022, Sanò et al, 2022). Some of them are based on radiative transfer simulations of observed snowfall events (Kongoli et al, 2003, Skofronick-Jackson et al, 2004, Kim et al, 2008), or on in-situ data (see Kongoli et al, 2015, Meng et al, 2017, Kongoli et al, 2018), others on CPR observations (Edel et al, 2020, You et al, 2022, Sanò et al, 2022), or a combination of them (Noh et al, 2009, Liu & Seo, 2013).*

to:

*The main novelty of the approach is the exploitation of the ATMS wide range of channels (from 22 GHz to 183 GHz) to obtain the radiometric characterization of the background surface at the time of the overpass. The derived surface emissivities are used to infer the clear-sky contribution to the measured TBs in the high frequency*

53 channels in the snowfall retrieval process. This approach is similar to the work of Zhao and Weng, 2002, for  
54 AMSU observations limited to non-scattering surfaces (i.e., ocean and vegetated land), however the application  
55 to surfaces with a very complex and time-varying emissivity (such as snow cover and sea ice) required a far-away  
56 more advanced algorithm taking advantage of machine learning techniques. Moreover, the algorithm is based  
57 on the exploitation of an observational dataset where each ATMS multichannel observation is associated with  
58 coincident (in time and space) CloudSat CPR vertical snow profile and surface snowfall rate (hereafter ATMS-  
59 CPR coincidence dataset).

60 Several snowfall retrieval algorithms for cross-track scanning radiometers have evolved in the last 20 years  
61 starting from the Advanced Microwave Sounder Unit-B (AMSU-B) (Zhao and Weng 2002, Kongoli et al, 2003,  
62 Skofronick-Jackson et al, 2004, Noh et al, 2009, Liu and Seo 2013), and Microwave Humidity Sounder (MHS)  
63 (see Liu & Seo, 2013, Edel et al, 2020), and evolving to ATMS (Kongoli et al, 2015, Meng et al, 2017, Kongoli et  
64 al, 2018, You et al, 2022, Sanò et al, 2022). Some of them are based on radiative transfer simulations of observed  
65 snowfall events (Kongoli et al, 2003, Skofronick-Jackson et al, 2004, Kim et al, 2008), or on in-situ data (see  
66 Kongoli et al, 2015, Meng et al, 2017, Kongoli et al, 2018), others on CPR observations (Edel et al, 2020, You et  
67 al, 2022, Sanò et al, 2022), or a combination of them (Noh et al, 2009, Liu & Seo, 2013).

68 The following reference has been added to the text (Line 810):

69

70 Zhao, L., & Weng, F.: Retrieval of ice cloud parameters using the Advanced Microwave Sounding Unit. *Journal*  
71 *of Applied Meteorology and Climatology*, 41(4), 384-395, <https://www.jstor.org/stable/26184983>, 2002.

72

73 Reference:

74

75 Zhao, L., & Weng, F.: Retrieval of ice cloud parameters using the Advanced Microwave Sounding Unit. *Journal*  
76 *of Applied Meteorology and Climatology*, 41(4), 384-395, <https://www.jstor.org/stable/26184983>, 2002.

77

78 **1.2) Line 67: replace with "new" or "latest"**

79

80 Thanks to the reviewer for the suggestion. The text has been modified

81 From:

82 *the availability of the last generation microwave radiometers*

83 to:

84 *the availability of the latest generation microwave radiometers*

85

86 **1.3) Line 89: Contrary to what's stated here, Greenland and Antarctica show scattering year-round in**  
87 **window and water vapor sounding channels, and even in the low temperature sounding channels.**

88

89 Thanks to the reviewer for the comment. Greenland and Antarctica have been defined as scatter-free by  
90 Grody&Basist, 1996. For what concerns our paper, the intention was to underline the absence of a significant  
91 difference between the emissivities at 23 GHz and at 31 GHz, typical of the snowcover over Greenland and  
92 Antarctic plateau (see Camplani et al, 2021), without referring to higher frequencies, as opposed to deep dry snow  
93 at lower latitudes where this difference is evident. So we agree that the term "scatter-free" can be misleading if  
94 we also consider high-frequency channels. Therefore, the text has been changed

95 from:

96 *At the same time, large areas of Greenland and Antarctica could appear as "scatter-free", although these areas*  
97 *throughout the year are covered by dry snowpacks.*

98 to:

99 *At the same time, large areas of Greenland and Antarctica, although these areas are covered by dry snowpacks*  
100 *throughout the year, do not show a significant difference between the two ATMS low frequency channels.*

101

102

103 References:

104 Grody, N. C., & Basist, A. N.: Global identification of snowcover using SSM/I measurements. *IEEE Transactions*  
105 *on geoscience and remote sensing*, 34(1), 237-249, DOI: 10.1109/36.481908, 1996.

106

107 Camplani, A., Casella, D., Sanò, P., & Panegrossi, G.: The Passive microwave Empirical cold Surface  
108 Classification Algorithm (PESCA): Application to GMI and ATMS. *Journal of Hydrometeorology*, 22(7), 1727-  
109 1744, <https://doi.org/10.1175/JHM-D-20-0260.1>, 2021.

110

111 **1.4) Lines 116-119: While 2CSP is a well-recognized product and is not derived from radiative transfer**  
112 **modeling, it does include assumptions about snow microphysics, and uses optimal estimation to retrieve**  
113 **these parameters. The algorithm also uses a simplified radar reflectivity equation. Refer to the 2CSP ATBD**  
114 **at [116 Thanks to the reviewer for the clarification. In the text, we wanted to highlight the issues inherent in using a  
117 dataset based on simulations \(cloud-resolving model and radiative transfer\) with respect to one based on  
118 coincident observations. The text has been changed](https://www.cloudsat.cira.colostate.edu/cloudsat-static/info/dl/2c-snow-profile/2C-SNOW-</a></b><br/>115 <b>PROFILE_PDICD.P1_R05.rev0_.pdf. Please modify the text here accordingly.</b></p></div><div data-bbox=)**

119 from:

120 *On the other side, the use of CPR-based datasets overcomes some of the limitations deriving from the assumptions*  
121 *to be made in cloud-radiation model simulations (e. g., the microphysics scheme, the emissivity of the background*  
122 *surface, scattering properties of ice hydrometeors), which are particularly problematic for snowfall estimation.*  
123 *However, some limitations of the radar product used as reference and issues related to the spatial and temporal*  
124 *matching between the CPR and the PMW radiometer measurements introduces some uncertainty.*

125 to:

126 *On the other hand, the use of CPR-based datasets overcomes some of the limitations deriving from the use of*  
127 *cloud-radiation model simulations, which are particularly challenging for snowfall events. However, some*  
128 *limitations of the radar product used as a reference and issues related to the spatial and temporal matching*  
129 *between the CPR and the PMW radiometer measurements introduce some uncertainty. Moreover, the 2CSP*  
130 *product is based on assumptions on snow microphysics, uses optimal estimation to retrieve snow parameters ,*  
131 *and uses a simplified radar reflectivity equation and is affected by CloudSat CPR limitations as outlined in*  
132 *Battaglia & Panegrossi, 2020.*

133

134 Reference:

135

136 Battaglia, A., & Panegrossi, G.: What can we learn from the CloudSat radiometric mode observations of snowfall  
137 over the ice-free ocean?. *Remote Sensing*, 12(20), 3285, <https://doi.org/10.3390/rs12203285>, 2020.

138

139 **1.5) Line 181: How is the underestimation of heavy snowfall handled in training and validating the SWP**  
140 **and SSR models?**

141 Thanks to the reviewer for the question. The aim of the algorithm is to reproduce the 2C-Snow Profile product  
142 snowfall climatology, which is the only global radar product obtained from satellites. So, the underestimation has  
143 not been corrected .

144 The following statement has been added to the text (line 223):

145 *Moreover, it is worth noting that CPR 2CSP product limitations for snowfall detection and estimation (see Section*  
146 *2.2) affect the algorithm snowfall retrieval capabilities.*

147

148

149 **1.6) Line 273: Do the ANNs use environmental parameters? What are they?**

150 Thanks to the reviewer for the question. The final version of the algorithm does not use environmental parameters  
151 as input of the ANNs, but only some ancillary parameters (Digital Elevation Model (DEM), radiometer viewing  
152 angle). So the text has been modified  
153 from

154 *Four ANNs are then applied to a predictor set consisting of ATMS  $T_{B_{obs}}$ ,  $\Delta T_{B_{obs-sim}}$ , a surface classification  
155 flag, and other environmental and ancillary parameters.*

156 to:

157 *Four ANNs are then applied to a predictor set consisting of ATMS  $T_{B_{obs}}$ ,  $\Delta T_{B_{obs-sim}}$ , a surface classification  
158 flag, and other ancillary parameters (elevation and ATMS viewing angle for the final version).*

159

160

161

162

163 **1.7) Lines 191-192: Add the info on the dataset's geographic area. Was the data filtered for high latitudes**  
164 **given the focus of this study?**

165

166 Thanks to the reviewer for the suggestion and for the question. The data have been not filtered based on a  
167 geographic criteria. However, the data selection is based on temperature ( $T_{2m} < 280$  K) and water vapor content  
168 ( $TPW < 10$  mm) and on elevation (see lines 320-321 and *Camplani et al, 2021*); As a consequence, the majority of  
169 the observations selected are obtained over high latitude areas. A statement about the dataset composition has  
170 been added (see answer to Comment 1.21).

171 Reference:

172

173 Camplani, A., Casella, D., Sanò, P., & Panegrossi, G.: The Passive microwave Empirical cold Surface  
174 Classification Algorithm (PESCA): Application to GMI and ATMS. *Journal of Hydrometeorology*, 22(7), 1727-  
175 1744, <https://doi.org/10.1175/JHM-D-20-0260.1>, 2021.

176

177 **1.8) Lines 193-194: With a 15-min time window, the snow mass that ATMS detects in the atmosphere most**  
178 **likely is higher than the near-surface snow (SSR) observed by CPR (refer to You et al., doi:**  
179 **10.1029/2019GL083426). This adds uncertainties to the SSR (and to a lesser degree to SWP). Suggest the**  
180 **authors run an experiment where ATMS data is collocated with CPR snowfall rate with a certain time lag**  
181 **(30-minute?), and compare the retrieved ATMS snowfall rate with what is presented in this manuscript.**

182

183 Thanks to the reviewer for the suggestion. The suggested experiment is extremely interesting, and we want to take  
184 it into account for future works. However, the selection of coincident observations and the making of a coincidence  
185 dataset is a computationally and time consuming process, so we do not have the possibility to face this problem  
186 during the revision phase. The following statement have been added to the conclusions (line 597):

187

188 *Moreover, recent studies have highlighted that TBs correlate more strongly with lagged surface precipitation*  
189 *(with a time lag of 30-60 min for snowfall) than the simultaneous precipitation rate ( see You et al, 2019) .*  
190 *Therefore, an analysis based on a coincident dataset characterized by different time lags will be carried out. The*  
191 *results of this analysis will be compared with HANDEL-ATMS performances in order to identify a way to exploit*  
192 *this information to improve SSR detection and estimation.*

193

194 The following reference has been added to the text (Line 806):

195

196 *You, Y., Meng, H., Dong, J., & Rudlosky, S.: Time-lag correlation between passive microwave measurements and*  
197 *surface precipitation and its impact on precipitation retrieval evaluation. Geophysical Research Letters*, 46(14),  
198 8415-8423, doi: 10.1029/2019GL083426, 2019.

199

200 Reference:

201  
202 You, Y., Meng, H., Dong, J., & Rudlosky, S.: Time-lag correlation between passive microwave measurements  
203 and surface precipitation and its impact on precipitation retrieval evaluation. *Geophysical Research Letters*,  
204 46(14), 8415-8423, doi: 10.1029/2019GL083426, 2019.

205  
206 **1.9) Line 282: Is there any noticeable discontinuity in the retrieved SWP and SSR between the different**  
207 **surface classes? Please add some discussion in the appropriate section.**

208  
209 Thanks to the reviewer for the comment. As it is possible to observe by the case study reported, discontinuities  
210 in the SWP/SSR retrieval are not observed in correspondence with the surface class change. Also for other case  
211 studies analyzed it has not been observed any discontinuity in snowfall retrievals in correspondence with a surface  
212 class change. In the following plots the statistical scores (POD, FAR and HSS) are reported as a function of the  
213 class. It is possible to observe that there are not very large differences. Also the error statistics do not show any  
214 significant difference between the various surface classes (see the answer to 1.23, Figure 9). So, the following  
215 statement has been added in the section dedicated to the case study (line 525):

216 *Discontinuities in snowfall retrievals are not observed in correspondence with surface class changes.*

217  
218 **1.10) Line 283: replace NASA with NOAA**

219 Thanks to the reviewer for the correction. The text has been modified

220 from:

221 *the NASA AutoSnow product*

222 to:

223 *the NOAA AutoSnow product*

224  
225 **1.11) Line 290: While this is outside the scope of this study, is it possible to improve snow cover classification**  
226 **using ML approach? I'd like to get the authors' comments on it.**

227 Thanks to the reviewer for the question. In *Camplani et al, 2021* a comparison between the PESCA performances  
228 and the performance obtained with a RobustBoost approach (Machine Learning ensemble method) has been  
229 carried out. The results show that the performances obtained with this ML approach are very similar to those  
230 obtained by using PESCA. However, the leading idea of PESCA is to use a simple and not too computationally  
231 demanding method to obtain a surface classification ancillary to the snowfall retrieval by exploiting the radiometer  
232 low-frequency channels. Indeed, in our opinion, the use of ML approaches for the prediction of the surface  
233 emissivity for snow cover surfaces is very promising. In particular, it could be of great benefit for the exploitation  
234 of the heterogeneous observations from the radiometer constellation. In this context, we are presently working in  
235 how the future measurements of CIMR radiometer, with an unprecedented spatial resolution, but no high  
236 frequency channels, can be exploited for improving the snowfall and IWP estimates of other radiometers equipped  
237 with high frequency channels, such as EPS-SG MWI, ICI, MWS the ATMS and AWS-STERNA. We sincerely  
238 thank the reviewer for this comment, and we would be pleased to further discuss this topic when the revision of  
239 this manuscript will be completed.

240 Reference:

241  
242 Camplani, A., Casella, D., Sanò, P., & Panegrossi, G.: The Passive microwave Empirical cold Surface  
243 Classification Algorithm (PESCA): Application to GMI and ATMS. *Journal of Hydrometeorology*, 22(7), 1727-  
244 1744, <https://doi.org/10.1175/JHM-D-20-0260.1>, 2021.

245  
246 **1.12) Line 327: give explicit definitions of POD, FAR, and HSS even though they are well known.**

247  
248 Thanks to the reviewer for the suggestion. The text has been modified

249  
250  
251 from:

252 The statistical scores (POD, FAR, HSS) of PESCA identification of sea ice and snow cover (using AutoSnow as  
253 reference) are summarized in Table 1.

254 to:

255 The statistical scores of PESCA identification of sea ice and snow cover (using AutoSnow as the reference) are  
256 summarized in Table 1. In particular, the Probability of Detection (POD), the False Alarm Ratio (FAR), and the  
257 Heidke Skill Score (HSS) are reported. POD, FAR, and HSS are defined by equations 2,3 and 4.

$$258 \text{POD} = \frac{h}{h+m}$$

259 (2)

$$260 \text{FAR} = \frac{f}{f+h}$$

261 (3)

$$262 \text{HSS} = \frac{2(h*cn-f*m)}{(h+m)*(m+cn)+(h+f)*(f+cn)}$$

263 (4)

264 where  $h$  represents the hits,  $f$  represents the false alarms,  $m$  represents the misses and  $cn$  represents the correct  
265 negatives

266

267 **1.13) Line 346: Give reference to the radiative transfer model, or add some information about the model.**

268

269 Thanks to the reviewer for the suggestion. The simulations are based on a plane-parallel approximation (see *Ulaby,*  
270 *2014*) and the gas absorption model is described by *Rosenkranz, 1998*. The text has been modified (see answer to  
271 Comment 1.15).

272 The following reference has been added to the text (Line 806):

273 *Rosenkranz, P. W., Water vapor microwave continuum absorption: A comparison of measurements and models.*  
274 *Radio Science, 33(4), 919-928. <https://doi.org/10.1029/98RS01182>, 1998.*

275 References:

276

277 *Ulaby, F., & Long, D., Microwave radar and radiometric remote sensing, 1st Edition, the Univ. of Michigan Press,*  
278 *ISBN: 978-0-472-11935-6, 2014.*

279 *Rosenkranz, P. W., Water vapor microwave continuum absorption: A comparison of measurements and models.*  
280 *Radio Science, 33(4), 919-928. <https://doi.org/10.1029/98RS01182>, 1998.*

281

282 **1.14) Line 350: Is the polarization effect on emissivity also neglected between viewing angles of 40 degree**  
283 **and 52.7 degree (the max ATMS viewing angle)? Need to state it if it's the case.**

284 Thanks to the reviewer for the question. The polarization effect is less than 0.05 between 0 ° and 52.7 °, so it has  
285 not been considered. In the plot below the dependence of the ocean emissivity on viewing angle at 89 GHz (top)  
286 and the differences between the emissivity at nadir and the emissivity at a certain angle (bottom) are reported  
287 based on the FASTEM model (see *Prigent et al, 2017*). It is possible to observe that, while the V and H emissivity  
288 show a variation up to 0.15, the QV and QH emissivity variation is lower than 0.05 for scan angles < 52 °.

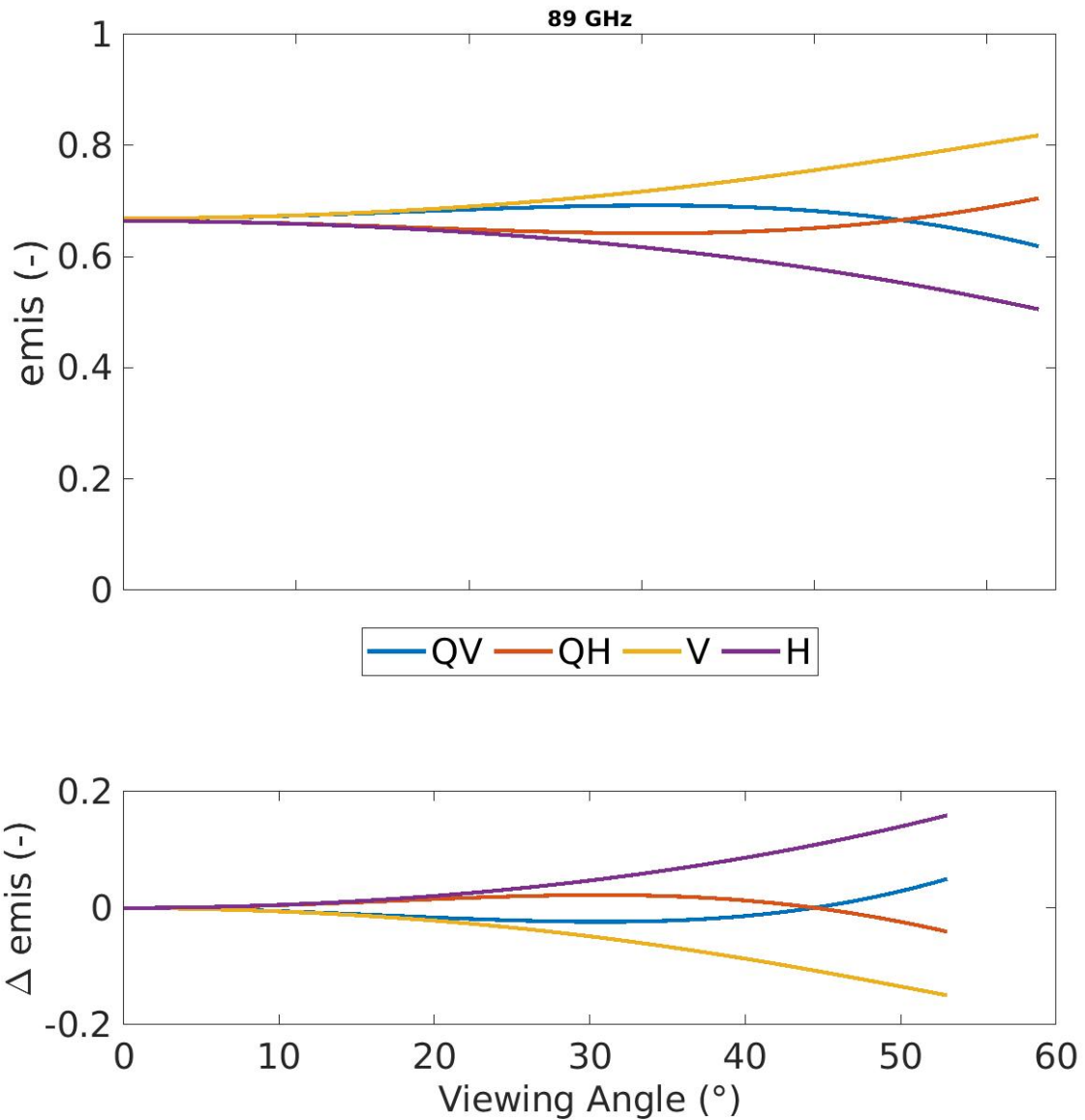
289 The text has been modified

290 from:

291 *The emissivity spectra dependence on the ATMS viewing angle for polarized surfaces has been neglected because*  
292 *an analysis of such dependence in the ATMS-CPR coincidence dataset has shown that it is significant only for*  
293 *larger viewing angles (tot for >40 °). This is due to the fact that cross-track scanning radiometers measure a*  
294 *signal (off-nadir) which derives from a mixture between the two polarizations (e.g., quasi-vertical, QV, and quasi-*  
295 *horizontal, QH). As a consequence, although the emissivities of polarized surfaces, such as open water surfaces,*  
296 *are strongly influenced by the viewing angle, for the cross-track scanning radiometers the emissivity variation is*  
297 *compensated by the effect of the mixture of the two polarization (see also Felde & Pickle, 1995, Prigent et al,*  
298 *2000, Mathew et al, 2008, Prigent et al, 2017).*

299 to:

300 *The emissivity spectra dependence on the ATMS viewing angle for polarized surfaces has been neglected because*  
301 *an analysis of such dependence in the ATMS-CPR coincidence dataset has shown that it is not significant for*  
302 *ATMS viewing angles (emissivity difference smaller than 0.05 for angles up to 52.7 °). This is due to the fact that*  
303 *cross-track scanning radiometers measure a signal (off-nadir) which derives from a mixture between the two*  
304 *polarizations (e.g., quasi-vertical, QV, and quasi-horizontal, QH). As a consequence, although the emissivities of*  
305 *polarized surfaces, such as open water surfaces, are strongly influenced by the viewing angle, for the cross-track*  
306 *scanning radiometers the emissivity variation is compensated by the effect of the mixture of the two polarization*  
307 *(see also Felde & Pickle, 1995, Prigent et al, 2000, Mathew et al, 2008, Prigent et al, 2017).*



308  
309

Reference:

Prigent, C., Aires, F., Wang, D., Fox, S., & Harlow, C.: Sea-surface emissivity parametrization from microwaves to millimetre waves. *Quarterly Journal of the Royal Meteorological Society*, 143(702), 596-605, <https://doi.org/10.1002/qj.2953>, 2017.

310

311

312 **1.15) Line 362: Reference for the RTM?**

313 Thanks to the reviewer for the suggestion. The text has been modified

314 from:

315 *The RMSE between simulated clear-sky TBs - based on the mean emissivity values estimated for each class - and*  
316 *the coincident observed clear-sky TBs appears to be too high to implement a robust signal analysis (>10 K).*

317 to:

318 *The clear-sky radiative transfer model simulations are based on the mean emissivity values estimated for each*  
319 *class, and simulated by using the plane-parallel approximation (Ulaby & Long, 2014) and the Rosenkrantz gas*  
320 *absorption model (Rosenkrantz, 1998) - The RMSE between simulated clear-sky TBs and the coincident observed*  
321 *clear-sky TBs appears to be too high to implement a robust signal analysis (>10 K).*

322

323 References:

324 Rosenkrantz, P. W., Water vapor microwave continuum absorption: A comparison of measurements and models.  
325 *Radio Science*, 33(4), 919-928. <https://doi.org/10.1029/98RS01182>, 1998.

326

327 Ulaby, F., & Long, D., Microwave radar and radiometric remote sensing, 1st Edition, the Univ. of Michigan Press,  
328 ISBN: 978-0-472-11935-6, 2014.

329

330 **1.16) Line 397, the RMSE for ocean is 3.37 K in Table 2.**

331

332 Thanks to the reviewer for the observation. The text has been modified

333 from:

334 very *low RMSE values ( $\approx 2$  K)*

335 to:

336 *low RMSE values ( $< 4$  K)*

337

338 **1.17) Line 403: Since high frequencies are more important for snowfall retrieval, need to discuss the impact**  
339 **of the significant uncertainties at these channels to retrieve SWP and SSR.**

340 Thanks to the reviewer for the suggestion. In Figure 9 (see answer to Comment 1.23) the statistical scores for  
341 each PESCA class are reported. It is possible to observe that the worst scores are obtained for classes characterized  
342 by high uncertainties in the clear-sky TB simulations (Perennial Snow, Winter Polar Snow). However, it is also  
343 worth noting that these classes are mostly associated with environmental conditions (very dry and cold, with very  
344 light snowfall events, see *Camplani et al, 2021*) which make it difficult both to obtain a more accurate clear  
345 emissivity estimation and to retrieve snowfall. At the same time, it can be observed that classes characterized by  
346 the highest uncertainties on the emissivity estimate (Deep Dry Snow and Broken Sea Ice), show statistical scores  
347 which are coherent with the general scores of the algorithm. So it is clear that the uncertainties on emissivity  
348 estimation have less influence than other factors, such as the environmental conditions.

349 The text has been modified (line 471)

350 from:

351 *In Table 6 the statistical scores of the algorithm performance by considering each PESCA class for both the SWP*  
352 *and the SSR detection module are reported. It can be observed that, also considering specifically the classes where*  
353 *the detection is more problematic, both for the uncertainties linked to the emissivity retrieval (see Table 2), for*  
354 *the extremely dry and cold environmental conditions, and for the low intensity of the snowfall events, such as*  
355 *Perennial Snow or Winter Polar Snow, HANDEL-ATMS has good detection capabilities (POD and FAR values*  
356 *greater than 0.7 and less than 0.25, respectively, for both SWP and SSR). These results provide evidence that*  
357 *HANDEL-ATMS can be used to analyze snowfall occurrence in the polar regions.*

358 to:

359 In Figure 9 the statistical scores of the algorithm performance by considering each PESCA class for both the  
360 SWP and the SSR detection module are reported. It can be observed that, also considering specifically the classes  
361 associated to extremely dry and cold environmental conditions such as Perennial Snow or Winter Polar Snow  
362 (see Camplani et al, 2021) (where the detection is more problematic due to the uncertainties in the emissivity  
363 retrieval (see Table 2), and to the low snowfall intensity), , HANDEL-ATMS has good detection capabilities (POD  
364 and FAR values greater than 0.7 and less than 0.25, respectively, for both SWP and SSR). On the other hand, it  
365 is possible to observe also that for surface classes characterized by the highest emission estimation uncertainties,  
366 such as Deep Dry Snow, the statistical scores are coherent with the general scores and better than those obtained  
367 in presence of extremely dry/cold environmental conditions. So, it is possible to conclude that the extremely  
368 cold/dry environmental conditions - have more influence on the detection than the uncertainties on clear sky  
369 emissivity estimation. Generally, these results provide evidence that HANDEL-ATMS can be used to analyze  
370 snowfall occurrence in the polar regions.

371

372 Reference:

373

374 Camplani, A., Casella, D., Sanò, P., & Panegrossi, G.: The Passive microwave Empirical cold Surface  
375 Classification Algorithm (PESCA): Application to GMI and ATMS. *Journal of Hydrometeorology*, 22(7), 1727-  
376 1744,<https://doi.org/10.1175/JHM-D-20-0260.1>, 2021.

377

378 **1.18) Line 430: Logarithmic tangent function is not a common activation function. Please add a reference**  
379 **or explain what it is.**

380 Thanks to the reviewer for this comment. It was a typo, the activation function is a sigmoid. We used hyperbolic  
381 tangent and sigmoid functions, which are indeed very common activation functions. The choice of the activation  
382 functions has been performed by trial and testing.

383 The manuscript has been modified

384 from:

385 *The final architecture, for all modules, is composed of four layers: an input layer with a neurons number equal*  
386 *to the predictor number, and a hyperbolic tangent function as the activation function, a first hidden layer (60*  
387 *neurons), and hyperbolic tangent function, a second hidden layer (30 neurons), with a logarithmic tangent*  
388 *function.*

389 to:

390 *The final architecture, for all modules, is composed of four layers: an input layer with a neurons number equal*  
391 *to the predictor number, and a hyperbolic tangent function as the activation function, a first hidden layer (60*  
392 *neurons), and hyperbolic tangent function, a second hidden layer (30 neurons), with a sigmoid function.*

393

394 **1.19) Lines 435-436: Did the predictor set including TB\_obs, TB\_obs-TB\_sim, and environmental variables**  
395 **give better result than the set only included the first two? If not, why? Is it because TB\_sim also used the**  
396 **environmental variables being tested?**

397 Thanks to the reviewer for the question. The NNs that use both the  $\Delta_{obs-sim}$  and the environmental parameters show  
398 detection scores almost equal to those obtained by using only  $\Delta_{obs-sim}$ . This is because the information about  
399 environmental conditions is already used as input in the clear-sky TB simulations The following statement has  
400 been added to the text (line 438):

401 *On the contrary, the simultaneous use of both the  $\Delta TB_{obs-sim}$  and the environmental parameters show scores almost*  
402 *equal to that obtained by using only  $\Delta TB_{obs-sim}$ .*

403

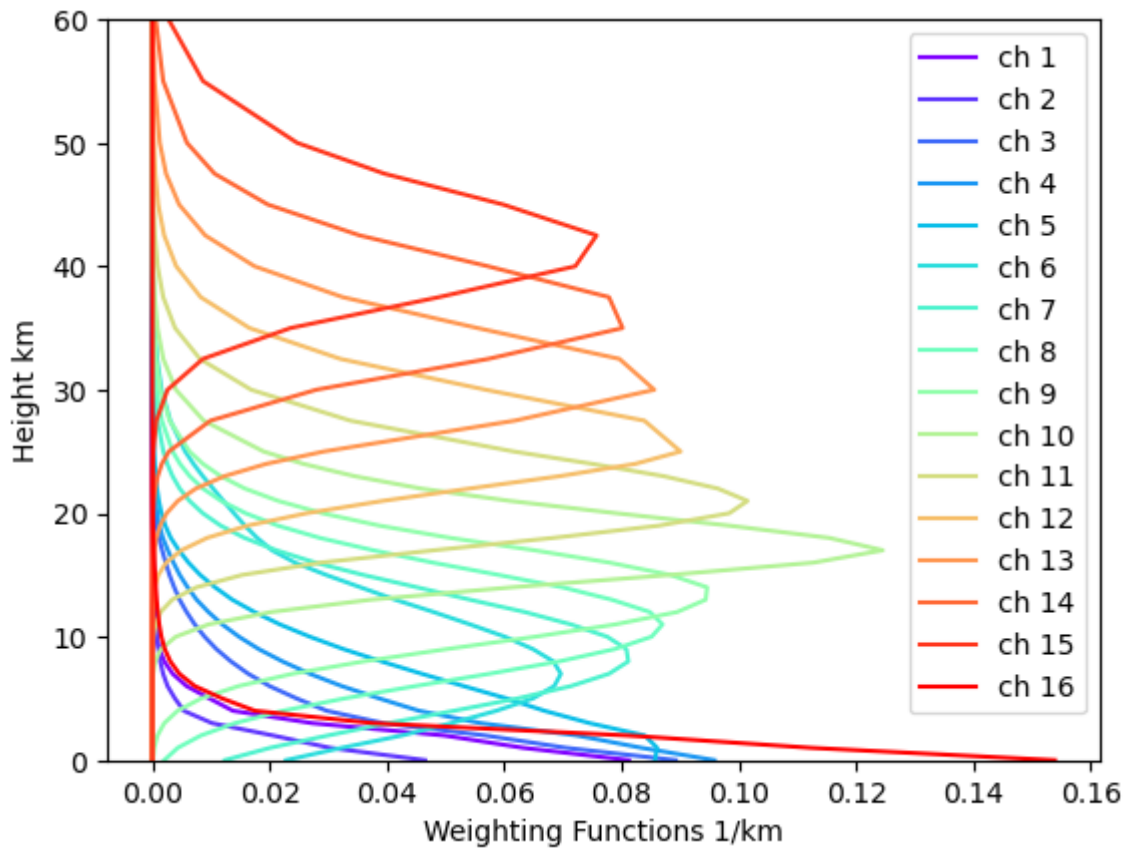
404

405

406 **1.20) Lines 444: Which 16 ATMS channels and how are they selected?**

407 Thanks to the reviewer for the suggestion. The sixteen channels are ATMS channels 1-9, 16-22. The ATMS 10-  
408 15 channels peak above the tropopause, so we did not take them into account in the development of HANDEL-

409 ATMS. Figure below shows the temperature weighting functions for a standard atmosphere in clear sky  
410 conditions.



411

412 The text has been modified

413 from:

414 *16 ATMS  $TB_{obs}$*

415 to:

416 *1-9, 16-22 ATMS channels  $TB_{obs}$  (the 10-15 ATMS channels have not been considered because their weighting  
417 function peaks above the tropopause).*

418

419 **1.21) Section 4.1: Some details about the validation data should be provided. Is the data from selected  
420 snowfall events used or from a time period? How many events were included and their geographic areas?  
421 How many data points were in the dataset etc.? The information is important because it provides the  
422 context for the performance metrics.**

423 Thanks to the reviewer for the suggestion. The following section has been added to the text of section 2.3 (line  
424 223):

425 *In this work, the dataset has been filtered based on humidity ( $TPW < 10$  mm) and temperature ( $T_{2m} < 280$  K) and  
426 elevation conditions (the working limits of the PESCA algorithm, see Camplani et al, 2021) leading to a good  
427 representation of the higher latitudes with 80 % of the dataset elements located above  $60^\circ N/S$  . The dataset is  
428 made of  $2,14 \cdot 10^6$  elements, including  $1,07 \cdot 10^6$  elements with falling snow ( $2CSP$   $SWP > 0$   $kg\ m^{-2}$ ) and  $9,99 \cdot 10^5$   
429 with snowfall at the surface ( $2CSP$   $SSR > 0$   $mm\ h^{-1}$ ) . The training and test phases have been conducted by  
430 splitting randomly the dataset, with  $\frac{1}{3}$  of the elements in the training and  $\frac{2}{3}$  of the elements in the test dataset.*

431

432 Reference:

433

434 Camplani, A., Casella, D., Sanò, P., & Panegrossi, G.: The Passive microwave Empirical cold Surface  
435 Classification Algorithm (PESCA): Application to GMI and ATMS. *Journal of Hydrometeorology*, 22(7), 1727-  
436 1744,<https://doi.org/10.1175/JHM-D-20-0260.1>, 2021.

437  
438

439 **1.22) Line 451: A large percentage of the snowfall appears to fall when T\_2m is around the freezing point**  
440 **or higher. Snowfall under such conditions generally has different characteristics from snowfall in high**  
441 **latitudes which is the focus of this study. Add some discussion about the data distribution and its impact on**  
442 **the new snowfall algorithm.**

443 Thanks to the reviewer for the suggestion. Generally, the SWP detection shows better performances in moister  
444 and warmer conditions than in colder/drier situations for two main reasons: 1) the atmosphere is less transparent  
445 2) these conditions are usually associated with more intense events. However, in these conditions there can be a  
446 mismatch between the presence of falling snow in the atmosphere and the presence of snowfall at the surface;  
447 therefore, the SSR detection statistical scores show a maximum around 273 K and 5 mm and then decrease. From  
448 Figure 8, it is possible to observe that the maximum number of observations and of snowfall elements in the  
449 dataset is around 273 K, where the best performances are obtained. However, it is worth noticing that HANDEL  
450 shows very good results also in very dry and very cold conditions. We believe that this is the main achievement  
451 of this work, since the main objective of this study is to show that HANDEL is able to detect and retrieve snow  
452 also in extreme conditions typical of the higher latitudes. We think that this is the added value of this study. In  
453 order to highlight this aspect, we have added a new figure showing the variability of the estimation statistical  
454 scores and the mean SWP and SSR with TPW (see answer to Comment 1.25).

455

456 **1.23) Line 471: Add HSS to Table 6.**

457

458 Thanks to the reviewer for the suggestion.

459 We have deleted Table 6 and we have added Figure 9, where the POD, FAR, HSS, the observation occurrences  
460 and the snowfall observation occurrences (SWP, SSR>0) are reported.

461

462

463

464

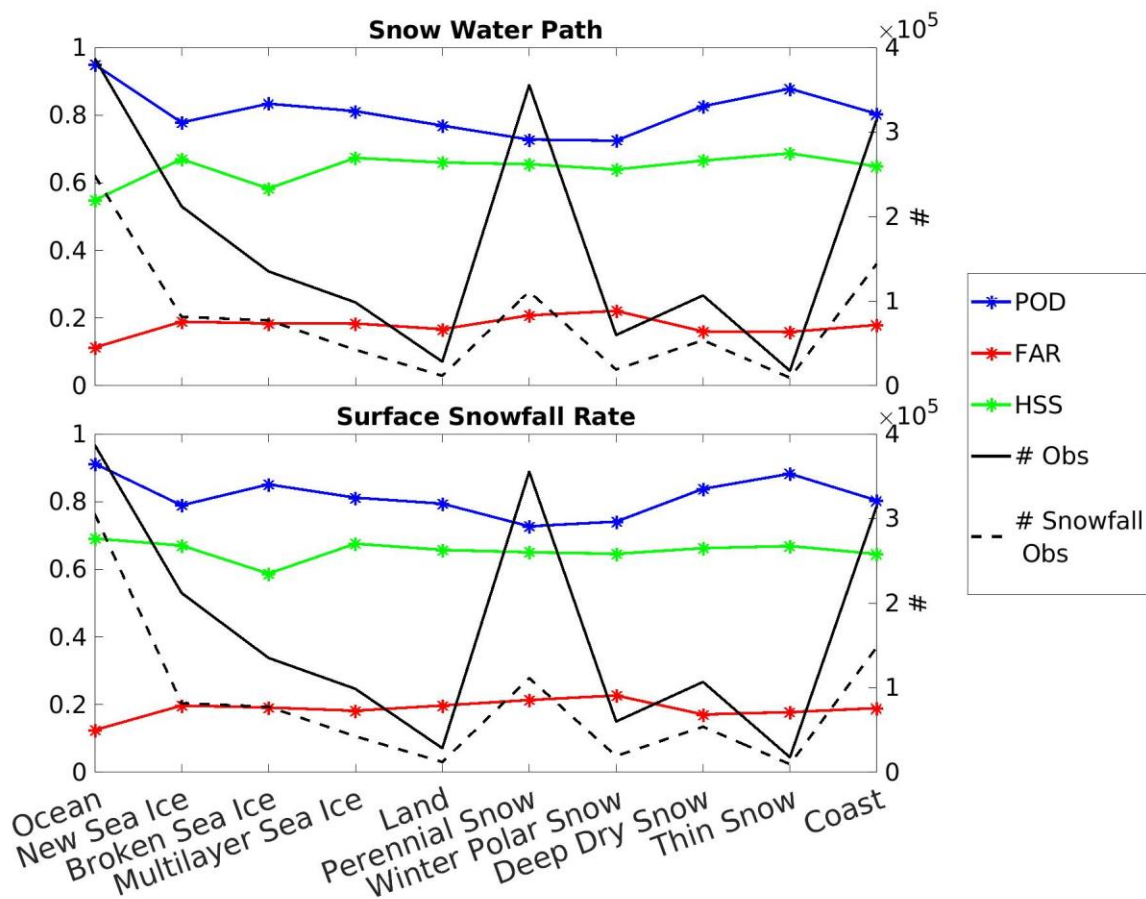


Figure 9: Same as Figure 7 but for PESCA surface classes.

465  
466  
467

1.24) Table 5: Since the goal of this study is to retrieve snowfall in high latitude, it'd be informative to analyze how well the statistics represent the cold, dry and light snowfall versus the warm, moist, and heavier snowfall. Please add some quantitative analysis to show the performance of the snowfall representative of high latitude conditions.

472 Thanks to the reviewer for the suggestion. The dependence of the detection scores on the environmental conditions has been reported in Figure 7 and in Figure 8. The presence of a less transparent atmosphere and the presence of high SWP values generates a more intense signal. We have decided to add one Figure in the manuscript showing the variability of the snowfall estimation statistical scores, as well as SWP and SSR, with TPW (see answer to Comment 1.25).

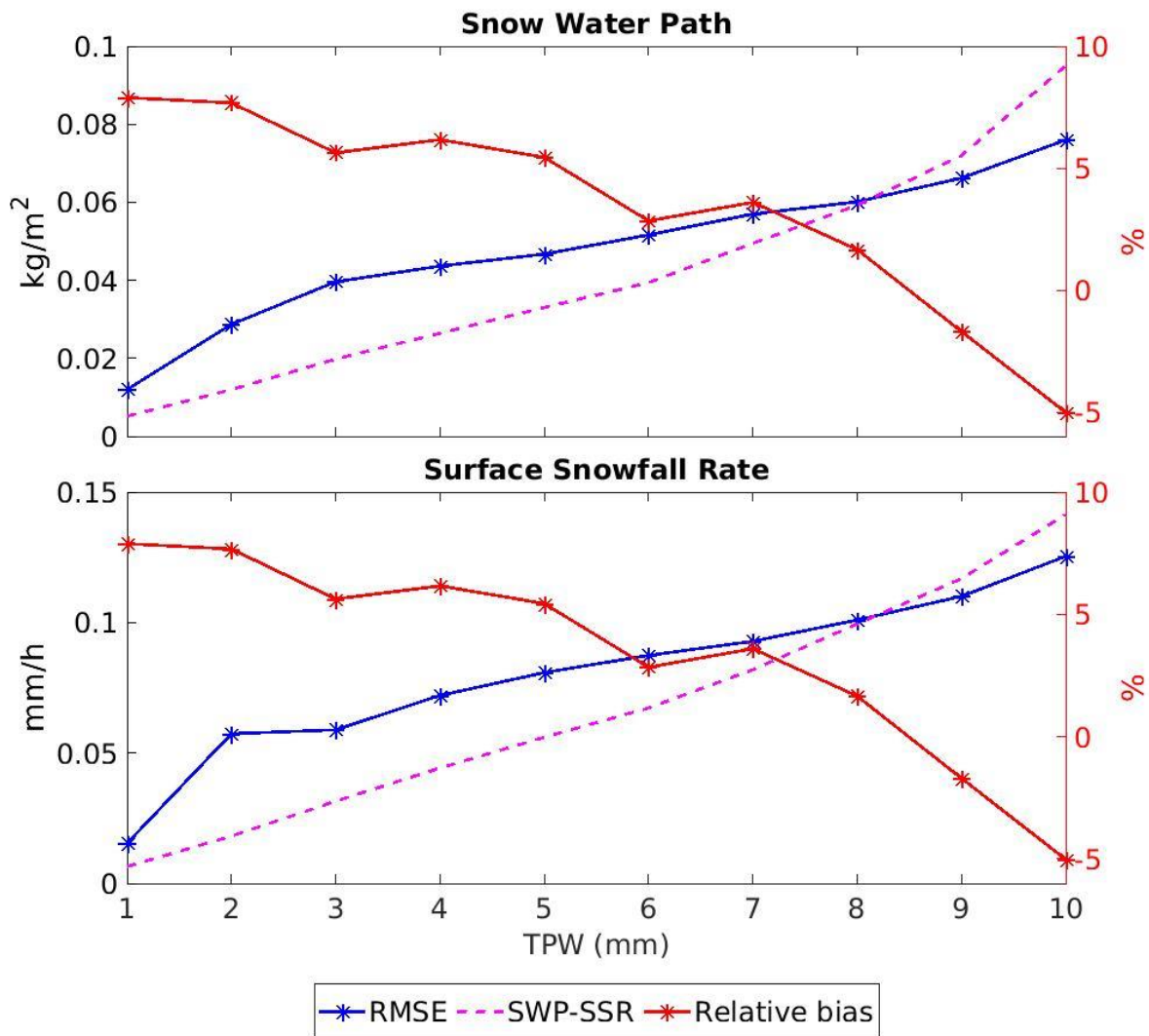
477

1.25) Line 487: Typically, high latitude snowfall is rather light. Does this result mean that the snowfall retrieval in high latitude is generally overestimated? Add some discussion here.

480 Thanks to the reviewer for the comment. From Figure 9 it is possible to observe that the algorithm tends to overestimate light snowfall, while there is a better agreement for more intense snowfall. Very light snowfall events are linked to the dry /cold environmental conditions typical of high latitude areas, where more intense snowfall events are typical of moister conditions. We state that "Generally, it can be observed that, although HANDEL-ATMS is able to detect extremely light snowfall events, it does not have the sensitivity to correctly estimate their intensity." The final part of Section 4.1 has been largely modified (see below)

486 We decided to add the following Figure to the paper in order to answer 1.22, 1.24 and 1.25.

487



488  
 489  
 490 *Figure 11: HANDEL-ATMS SWP and SSR Detection Performances for different bins of TPW. The left y-axis*  
 491 *reports RMSE absolute values and the mean intensity value for each 1-mm TPW bin, while the relative bias,*  
 492 *calculated as the ratio between the bias and the SWP/SSR mean value for each bin.*  
 493  
 494

495 The text has been modified to comment the Figure 11 (Line 488)

496 from:

497 . Generally, it can be observed that, although HANDEL-ATMS is able to detect extremely light snowfall events, it  
 498 does not have the sensitivity to correctly estimate their intensity.

499  
 500 to:

501  
 502 *Figure 11 shows the dependence of HANDEL-ATMS snowfall estimation error statistics, as well of SWP and SSR,*  
 503 *on TPW. The curves represent the mean SWP or SSR computed for each 1-mm TPW bin, the RMSE and the relative*  
 504 *bias (the ratio between the bias and the SWP/SSR mean value for each bin). TPW and snowfall intensity are*  
 505 *strongly correlated. An increase of the absolute RMSE can be observed as TPW increases, and it is larger than*  
 506 *the SWP/SSR mean value for TPW < 8 mm. A similar behavior can be observed by analyzing the dependence of*

507 *HANDEL-ATMS snowfall estimation error statistics on  $T_{2m}$  (not shown). A very moderate overestimation is*  
508 *observed for  $TPW < 8$  mm and for lower SWP and SSR values ( $< 0.1$  mm/h), with relative bias around 5%, (up*  
509 *to 8% only for extremely low TPW values and very low number of observations (see Figure 7)), while*  
510 *underestimation (relative bias up to -5%) is observed for higher TPW values and higher SWP and SSR values.*  
511 *Generally, light snowfall events are linked to the very cold/dry environmental conditions typical of high-latitude*  
512 *regions. So, the algorithm manages to detect also the very light snowfall typical of high latitudes, but tends to*  
513 *slightly overestimate snowfall intensity in such conditions. It can be concluded that HANDEL-ATMS has good*  
514 *detection capabilities (also for extremely light snowfall) but it shows some limitations in correctly estimating its*  
515 *intensity, with slight overestimation of the very light snowfall typical of high latitudes.*

516

517 **1.26) Lines 555-558: See the comment on line 27.**

518

519 Thanks to the reviewer for the suggestion. The text has been modified

520 from:

521

522 *The driving and innovative principle in the algorithm development is the exploitation of the full range of ATMS*  
523 *channel frequencies to characterize the frozen background surface radiative properties at the time of the overpass*  
524 *to be able to better isolate and interpret the snowfall-related contribution to the measured multi-channel upwelling*  
525 *radiation.*

526 to

527

528 *The driving and innovative principle in the algorithm development is the exploitation of the full range of ATMS*  
529 *channel frequencies to characterize the frozen background surface radiative properties at the time of the overpass*  
530 *to be able to better isolate and interpret the snowfall-related contribution to the measured multi-channel upwelling*  
531 *radiation. A similar approach has been used by Zhao & Weng, 2002; however, their application was limited to*  
532 *non-scattering surfaces and was based on empirical relationships.*

533

534 Reference:

535

536 Zhao, L., & Weng, F.: Retrieval of ice cloud parameters using the Advanced Microwave Sounding Unit. *Journal*  
537 *of Applied Meteorology and Climatology*, 41(4), 384-395, <https://www.jstor.org/stable/26184983>, 2002.